

Highly-Efficient Binary Neural Networks for Visual Place Recognition

Bruno Ferrarini¹, Michael Milford², Klaus D. McDonald-Maier¹ and Shoaib Ehsan¹

Abstract—VPR is a fundamental task for autonomous navigation as it enables a robot to localize itself in the workspace when a known location is detected. Although accuracy is an essential requirement for a VPR technique, computational and energy efficiency are not less important for real-world applications. CNN-based techniques archive state-of-the-art VPR performance but are computationally intensive and energy demanding. Binary neural networks (BNN) have been recently proposed to address VPR efficiently. Although a typical BNN is an order of magnitude more efficient than a CNN, its processing time and energy usage can be further improved. In a typical BNN, the first convolution is not completely binarized for the sake of accuracy. Consequently, the first layer is the slowest network stage, requiring a large share of the entire computational effort. This paper presents a class of BNNs for VPR that combines *depthwise separable factorization* and *binarization* to replace the first convolutional layer to improve computational and energy efficiency. Our best model achieves state-of-the-art VPR performance while spending considerably less time and energy to process an image than a BNN using a non-binary convolution as a first stage.

I. INTRODUCTION

Mobile robots need to track their position within the workspace to operate autonomously. As part of the navigation system, place recognition is fundamental in the localization process. It enables a robot to localize itself in the environment when a previously visited place on the map is detected. The rapid improvements in vision sensing capabilities made cameras the primary source of information for many robotics platforms motivating the interest in addressing place recognition with visual information [35], [33]. Visual Place Recognition (VPR) primarily consists of matching the current camera view with an internal representation of the environment (a map) to determine the current robot’s location. The changes occurring in an environment such as illumination, weather variations, and the different angles from which the camera captures a place render VPR an arduous endeavor. Convolutional Neural Networks (CNNs) are successfully employed in VPR applications achieving state-of-the-art performance under intense appearance changes [53]. However, CNNs have high runtime requirements unaffordable for many small robots [34], [19]. Binary neural networks (BNN) [13]

This work was supported by the UK Engineering and Physical Sciences Research Council through grants EP/R02572X/1, EP/P017487/1, and in part by the RICE project funded by the National Centre for Nuclear Robotics Flexible Partnership Fund.

¹Bruno Ferrarini, Klaus D. McDonald-Maier and Shoaib Ehsan are with the School of Computer Science and Electronic Engineering, University of Essex, Colchester, CO4 3SQ, UK {bferra, kdm, sehsan}@essex.ac.uk

²Michael Milford is with the QUT Centre for Robotics, School of Electrical Engineering and Robotics, Brisbane, QLD 4000, Australia, and was partially supported by the QUT Centre for Robotics. michael.milford@qut.edu.au

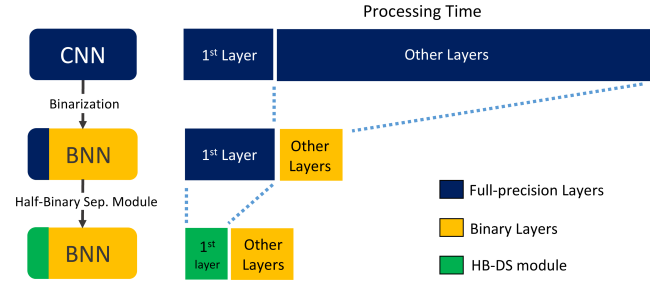


Fig. 1. In a typical BNN the first layer is not binarized for better accuracy. Hence, it is responsible for a significant part of the entire processing time. HB-DS module is a computationally efficient drop-in replacement to solve such a bottleneck problem in BNNs.

are a more efficient yet effective alternative to CNNs for enabling VPR in resource-constraint contexts [18]. BNNs use a single bit to encode weights and activations, allowing compact model sizes and bitwise operations to achieve high computational efficiency [26]. Although a BNN can be one order of magnitude faster than a CNN, there is a substantial margin for improvement. For better classification and VPR accuracy, the first layer of BNNs takes high precision inputs [26], [18]. Hence, the first convolution is incompatible with bitwise operations resulting in the most inefficient stage of a BNN, as exemplified in Fig. 1. Such a bottleneck problem is particularly relevant for VPR as many techniques use a relatively small number of convolutions [18], [36], [7], [12], [49]. Therefore, the first layer computes a significant part of the total operations to process an image that cannot be binarized without impacting the VPR performance.

This paper addresses the efficiency bottleneck of the first convolutional layer in BNNs by proposing the *Half-Binary Depthwise Separable* (HB-DS) module. HB-DS combines depthwise separable factorization [43], [25] with binarization to enhance the computational efficiency of a BNN without affecting the VPR performance. The HB-DS module is then used to design a BNN that can be tuned to train models with several levels of efficiency to meet different application requirements. Our best model achieves state-of-the-art performance requiring considerably lower resources than several VPR techniques regarded as highly efficient. For example, our network requires 50% of the time and energy spent by FloppyNet [18], a BNN for VPR, and it is four times faster than CALC [36], a small-factor CNN proposed to address loop closure detection efficiently.

The rest of this paper is organized as follows. Section II presents the related work. Section III describes the HB-DS module and the proposed network. The experimental setup

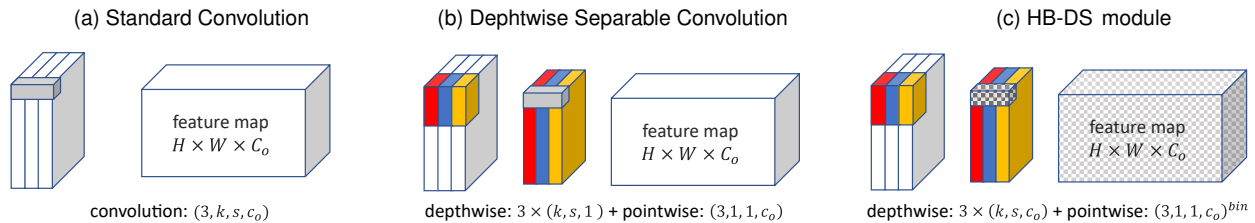


Fig. 2. A standard convolution works on all the inputs channels simultaneously to compute a feature map (a); depthwise separable factorization splits a convolution into depthwise and pointwise layers (b); half-binary separable convolution uses a binary pointwise convolution (c).

and evaluation criteria are described in Section IV. Section V presents and discusses the experimental results. Conclusions are drawn in Section VI.

II. RELATED WORK

A. Visual Place Recognition

Solving the VPR problem is the key to enable a robot to operate autonomously in a workspace. Despite the attention received and the significant advances in recent years, VPR remains challenging due to the viewpoint and appearance changes a robot encounters in real-world applications. Among the most effective VPR techniques are those using CNNs, which achieve the highest performance in dynamic environments [53], [50], [54]. The features computed by a CNN can be used as an image descriptor to match place images. A pre-trained AlexNet model [30] on Imagenet [41] is used for loop-closure detection [24], [7] and for enhancing the viewpoint tolerance of SeqSLAM [37], [16]. AMOSNet and HybridNet [11] are CNN trained on Specific Places Dataset (SPED) [11] with the aim to compute specific descriptors for place images. Zhou *et al.* followed the same idea proposing Place365 [55], a large place dataset used to train several CNNs, including VGG-16 [45], to solve the VPR problem in changing environments. CNN features can be post-processed to compute a robust and compact image descriptor. R-MAC [49] applies a max pooling schema to the last convolutional layer of a pre-trained CNN and aggregates the resulting features into a vectorized image descriptor. Cross-Region-Bow [12] and Regional-VLAD [29] identify regions-of-interest (ROIs) in a pre-trained CNN's feature map and aggregate the underlying features using Bag-of-Visual-Words (BoW) [39] and VLAD [28], respectively. Unlike the others two-stage techniques, NetVLAD [5] trains the CNN and subsequent modules end-to-end to obtain a VLAD-like descriptor highly tolerant to viewpoint variations.

Although effective for VPR, CNNs are computationally intensive. CALC [36] is an attempt to reduce the runtime requirement for VPR. It consists of a lightweight CNN trained using an autoencoder to recreate a HOG [15] descriptor from geometrically distorted place images. CoHOG [51] is a trainingless methods proposed as a computationally efficient alternative to CNNs. It detects regions of interest using image-entropy [52] that are subsequently assigned with a HOG descriptor to form an image representation. Neurological-inspired techniques are considered as well to

address VPR efficiently. FlyNet+CANN [10] uses a compact pattern recognition stage followed by a time filter to match image sequences. DrososNets [6] consists of an ensemble of compact bio-inspired place classifiers connected to a voting systems to determine the correct match with the camera's view. Binary neural networks (BNNs) [13] use 1-bit parameters and bitwise arithmetic to speed-up convolution and reducing dramatically the memory usage. FloppyNet [18] is a recently proposed BNNs for VPR applications. Its three-layer structure, along with bitwise arithmetic, makes FloppyNet a compact and computationally efficient image feature extractor. In this paper we propose a BNN with the same VPR accuracy as FloppyNet but substantially higher computational and energy efficiency.

B. Binary Neural Networks

CNNs successfully address the VPR problem but requires a heavy computational effort to build an image representation [19], [34]. Improving CNNs efficiency is a challenging task that received significant attention in the last decade. The earliest approaches reduce the computational complexity by pruning redundant connections and weights in trained models [32], [23], [22]. Post-training quantization is another method to reduce the computational requirements of a CNN. While post-quantization works reasonably well with eight or more bits in practical cases [3], post-binarization affects the performance of a model dramatically [14]. Binary-aware training is necessary to enable BNNs with good classification accuracy [44]. Training a binary model was attempted decades ago [42]. However, only after introducing the Straight-Trough-Estimator (STE) method [9], binary-aware training becomes easy to implement with gradient-based techniques. STE has become a standard in BNNs training. It is supported by an increasing number of machine-learning frameworks, including Larq [21] and Brevitas [38].

Since the first BNN trained with STE [13], several additions to the field were made. XNOR-Net [40] places max-pooling layers before the quantization function to prevent pooling from binarized features that would result in a non-informative map overpopulated by *ones*. Tang *et al.* [48] learn a positive gain to apply to negative values to prevent frequent binary weight oscillations to ensure a shorter training and better performance. In [17] the binarization threshold is a learnable parameter for better classification accuracy. The application of BNN to VPR is investigated in [18]. Training a model using a fully connected stage including

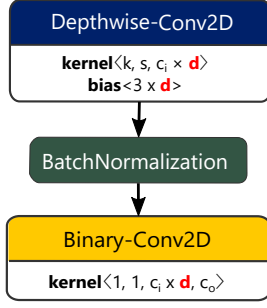


Fig. 3. HB-DS module implementation. d denotes the depth multiplier, k the kernel size, s the stride, c_i and c_o the input and out channels, respectively.

only full-precision neurons improves a model’s performance when convolutional features are used for VPR.

An open problem in BNNs concerns the first convolutional layer, which is not binarized in most state-of-the-art BNNs to avoid performance loss [44], [4]. Consequently, the first convolution is incompatible with bit-wise operations resulting in the slowest stage of a binary network (Section V-C). This paper proposes HB-DS, a module to replace the first convolutional layer to reduce the processing time of BNNs without affecting the VPR accuracy.

III. SOLVING THE FIRST LAYER BOTTLENECK PROBLEM

The first convolutional layer is crucial for a BNN’s performance. A common practice in BNN design is using high-precision inputs because binarization negatively affects performance [26]. Consequently, the first convolutional layer is incompatible with bit-wise operations resulting in the slowest stage of a BNN. For example, this is the case of FloppyNet [18], a recently proposed BNN designed for VPR applications consisting of three convolutions and three max-pool layers. The first FloppyNet’s convolution takes approximately 84% of the total processing time, as detailed in Section V-C.

This section presents the *Half-Binary Depthwise Separable* module (HB-DS), to solve the first layer bottleneck problem. Then we use it to design a highly efficient BNN. The HB-DS module and the proposed BNN are detailed below.

A. Depthwise Separable Convolutions

Our approach uses depthwise separable factorization to split a convolution into two separate layers: a depthwise convolution and a pointwise convolution [43], [25]. Depthwise convolution convolves the input channels individually. The input is convolved without changing the depth. Hence, the resulting feature map has the same channels as the input. The pointwise layer consists of a 1×1 convolution that builds a new map from the depthwise layer’s features. Fig. 2 shows the idea underlying depthwise separable decomposition.

The term complexity is used here as a synonym for the number of multiply-accumulate operations (MACs) computed by a convolution. Hence, lower computational complexity means fewer MACs. Let us assume a convolutional

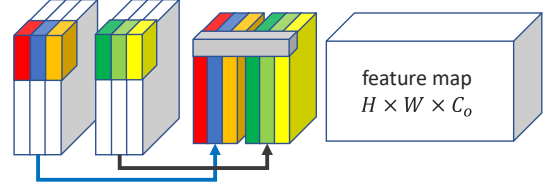


Fig. 4. Depthwise separable factorization with a depth multiplier of 2.

layer takes an input tensor $T_{in} = h_i \times w_i \times c_i$ and uses a kernel, $k \times k$, to output a feature map $T_{out} = h_o \times w_o \times c_o$. The computational cost is:

$$C_{conv} = (k^2 \cdot c_i) \cdot h_o \cdot w_o \cdot c_o, \quad (1)$$

where $(k^2 \cdot c_i)$ is the cost for a single element in T_{out} .

A depthwise convolution convolves the input channels individually, creating a feature map having the same depth, c_i , as the input tensor. Fig. 2.b shows an example of a depthwise convolution processing a three-channel tensor (e.g. a color image). The computational cost of a depthwise convolution is as follows:

$$C_{depth} = k^2 \cdot c_i \cdot h_o \cdot w_o. \quad (2)$$

The subsequent pointwise stage is a standard convolution with $k = 1$:

$$C_{point} = c_i \cdot h_o \cdot w_o \cdot c_o, \quad (3)$$

The total computational cost of a depthwise separable convolution is:

$$C_{sep} = C_{depth} + C_{point} = c_i \cdot h_o \cdot w_o \cdot (k^2 + c_o). \quad (4)$$

Compared to a standard convolution, the depthwise separable factorization reduces the complexity by:

$$\frac{C_{conv}}{C_{sep}} = \frac{k^2 c_o}{c_o + k^2}. \quad (5)$$

The larger the kernel, more effective is the depthwise separable factorization.

B. Half-Binary Depthwise Separable Convolutions

We proposed a half-binary variant of depthwise separable factorization where only the second layer resulting from the decomposition is binarized (Fig. 2.c). Hence, the depthwise layer takes full precision inputs while the subsequent pointwise convolution is binary for higher computational efficiency. The share of binary MACs is:

$$\frac{C_{point}}{C_{sep}} = \frac{c_o}{k^2 + c_o}. \quad (6)$$

Conversely, the full precision MAC are those in the depthwise convolution:

$$\frac{C_{depth}}{C_{sep}} = \frac{k^2}{k^2 + c_o}. \quad (7)$$

If $c_o > k^2$ the effect of binarization is dominant on factorization. Conversely, the complexity reduction is primarily due to factorization.

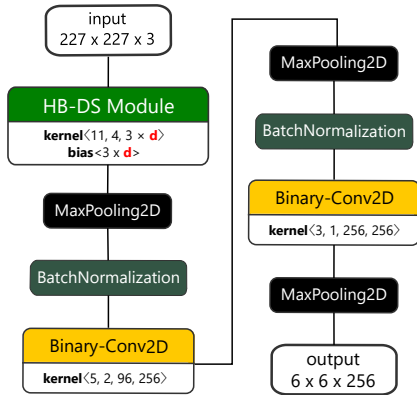


Fig. 5. The proposed BNN uses HB-DS as a first stage. d denotes the depth multiplier.

The implementation of the HB-DS module is illustrated in Fig. 3. A batch normalization layer [27] is placed before the binary convolution to improve a model’s accuracy and training speed [4].

Depthwise convolution can apply multiple kernels to an input channel creating a thicker feature map. Let d denotes the *depth multiplier*. The resulting feature map has $d \cdot c_i$ channels, as exemplified in Fig. 4 for $d = 2$. The application of a depth multiplier increases the computational complexity of HB-DS by d times. Therefore, Eq. 5 is rewritten as follows:

$$\frac{C_{conv}}{C_{sep}} = \frac{k^2 c_o}{d(c_o + k^2)}. \quad (8)$$

On the other hand, the VPR performance of a BNN improves as d increases. Section V-C demonstrates the use of d as a tuning parameter to adapt a model to different hardware capabilities while keeping HB-DS faster than an ordinary convolutional layer.

C. Network Architecture

The proposed network shown in Fig. 5 is inspired by FloppyNet. The HB-DS module uses a 11×11 kernel, stride of 4 and has 96 output channels. The rest of the network includes two pairs of binary convolution-max pooling blocks. The binary convolutions do not use bias but are preceded by batch normalization. The output features are from the last pooling layer.

IV. EXPERIMENTAL SETUP

The proposed network is trained with several depth multipliers, d . The resulting models are assessed on VPR under various environmental changes. A model’s efficiency is evaluated using processing time and energy usage as criteria.

A. Training Data

All the binary models are trained from scratch using Place365 [55] within the Larq framework [21]. Places365 is a place-themed dataset consisting of 1,803,460 images divided into 365 classes, including between 3068 and 5000 samples. The validation set includes 100 images per category.

TABLE I
TEST DATASETS AND GROUND TRUTH TOLERANCE.

Dataset	Condition	Reference Images	Query Images	Ground Truth
GardenPoints	Lateral Shift; Night-Day.	201	201	2 frames
SPED	Weather; Night-Day.	1000	200	5 frames
RobotCar Cross-Seasons	Lateral Shift; Illumination; Dynamic Elements.	203	180	± 5 frames
Nordland	Seasons.	1622	1622	5 frames
Old City	Strong 6-DOF.	5408	5643	by authors
Combined	All above.	8434	1000	Mixed

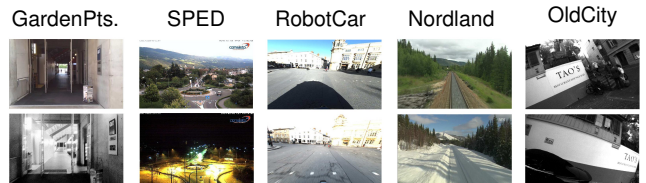


Fig. 6. A matching pair from every test dataset.

B. Test Data

VPR assessment is carried out under different image variations that a robot encounters over extended runs. The test data is divided into five datasets, each containing one or more image changes. They include: GardenPoints [47], 200 places randomly sampled from SPED [11], the Cross-Season sequence from RobotCar [31], Nordlands [46] and Old City [35]. Table I summarizes the characteristics and the ground truth criteria for each dataset. All of them include a reference set representing the knowledge of the environment and a query set representing the current view of a robot’s camera. Fig. 6 shows some examples of matching pairs.

We included a sixth dataset, Combined, to simulate a large complex environment. The reference set is the union of the other five datasets; the query set includes 200 randomly sampled images for a total of 1000 queries. The Combined dataset is intended to provide more realistic global performance measures than averaging the results from five datasets tested individually.

C. Evaluation Criteria

1) *VPR Performance*: VPR is cast as a loop closure detection problem. A query image representing the current robot’s camera view is compared to the reference images showing the previously visited locations. The image descriptor for our model is obtained from the vectorized output of a convolutional or pooling layer by L2-normalization:

$$D = \frac{\hat{X}_l}{\|\hat{X}_l\|_2}, \quad (9)$$

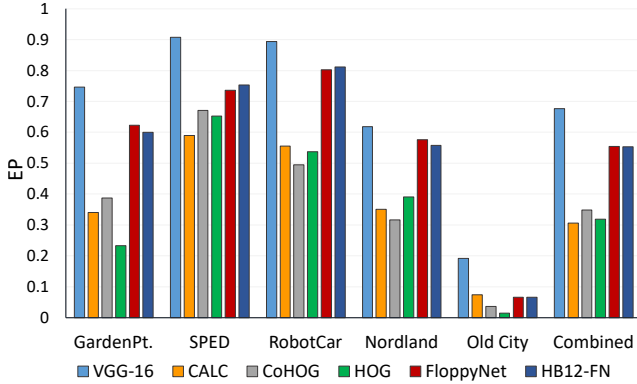


Fig. 7. VPR performance on different environmental conditions.

where \hat{X}_l is the output of the l^{th} layer. The similarity between the two images is determined using cosine:

$$\cos(\psi) = \frac{D_1 \cdot D_2}{\|D_1\| \cdot \|D_2\|}. \quad (10)$$

The reference image scoring the highest similarity with the query is regarded as the current location. VPR performance is measured on a dataset using several criteria including the percentage of true positive matches (TP%) and two metrics computed from Precision-Recall curves: Extended Precision (EP) [20] and AUC. EP extends the recall at 100% precision (R_{P100}) [16] to the lower spectrum by incorporating the precision at the minimum recall (P_{R0}):

$$EP = \frac{P_{R0} + R_{P100}}{2}. \quad (11)$$

EP is in $[0, 1]$: higher the value, better the VPR performance.

2) *Processing Time and Energy Usage*: The processing time, T_i , and power usage, P_w are acquired from deployed models and techniques running on a test hardware platform. T_i is the time required to elaborate an input image. The image loading and preprocessing (e.g. reshaping) are excluded so that T_i reflects the actual computational complexity of a VPR technique.

The energy per image processed, E_i , indicates the energy spent to compute a single image representation. It is determined from the power usage as follows:

$$E_i = P_w \cdot T_i, \quad (12)$$

where P_w is the power absorbed during image processing.

V. RESULTS DISCUSSION

This section presents the results for the proposed BNN discussing both the VPR performance and efficiency. The experiments include several implementations of our BNN using different depth multipliers, d (Section III-B). By convention, HBX-FN denotes a binary model using HB-DS with $d = X$. The computational time and energy usage are measured from deployed models. We used Larq-Compute-Engine (LCE) [8] to run binary models on a Raspberry Pi4 (RPI4) [2].

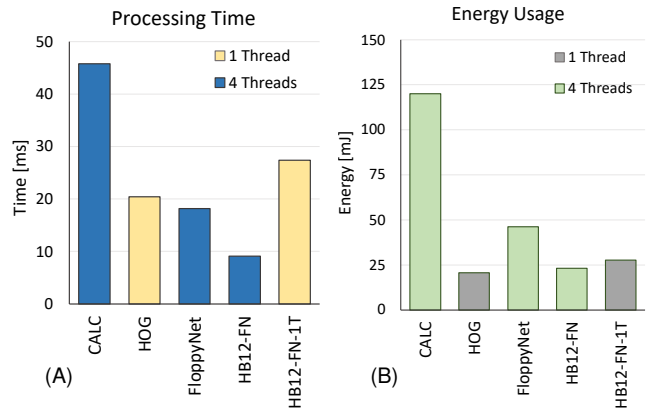


Fig. 8. Processing time (A) and energy usage (B) of the proposed BNNs compared to other VPR methods.

In the first part of this section, we compare HB12-FN to other VPR techniques. We selected HB12-FN as the best-balanced model between computation and performance. However, the experiments involved multiple models trained with different d values. The second part of this section presents the relative results and discusses d as a tuning parameter.

A. Comparative Analysis

The VPR networks and methods included in the comparison are FloppyNet [18], VGG-16 [45], CALC [36], CoHOG [51] and HOG [15]. To the best of our knowledge, FloppyNet is the only BNN designed for VPR. Thus, we consider it as a baseline comparison for HB12-FN. VGG-16 is a large CNN used in several state-of-the-art VPR applications [5], [12], [49]. It includes 13 convolutions and computes about 15M MACs to obtain an image representation from its last convolutional layer. The VGG-16 model used for the experiment is optimized on Place365. As opposed to VGG-16, CALC is a lightweight CNN designed to address VPR efficiently. We used the model trained on Place365 shared by the authors. CoHOG is proposed as an efficient and training-less alternative to CNNs. For the experiments, we used the source code and the parameters shared by the authors for an image size of 256×256 pixels [1]. Finally, HOG is used for

TABLE II
VPR METRICS ARE GIVEN FOR THE COMBINED DATASET. T_i AND E_i ARE MEASURED ON A RASPBERRY PI4.

VPR	Type	T_i [ms]	E_i [mJ]	VPR (combined)		
				EP	AUC	TP[%]
VGG-16	CNN	995.7	2608.7	0.676	0.679	80.5
CALC	CNN	45.8	120	0.306	0.323	37.1
CoHOG	Trainless	87.4	210.6	0.349	0.37	42.5
HOG	Trainless	20.4	20.6	0.318	0.335	38.6
FloppyNet	BNN	18.2	46.2	0.554	0.568	67.3
HB12-FN	BNN	9.1	23.1	0.553	0.566	67.2
HB12-FN-1T	BNN	27.4	27.7	0.553	0.566	67.2

TABLE III

PERFORMANCE AND EFFICIENCY FOR SEVERAL IMPLEMENTATION OF THE PROPOSED BNN. T_i AND E_i ARE MEASURED ON A RASPBERRY PI 4.

BNN	First Stage						T_i [ms]		E_i [mJ]	VPR (Combined Dataset)		
	Structure (k, s, c_o, d)	d	Params		MAC [M]					First	Total	EP
			32 bit	1 bit	32bit	1bit						
HB1-FN	C(11,4,96)	1	372	288	1.1	0.9	2.4	5.6	14.2	0.442	0.458	53.2
HB4-FN	HD-BS(11,4,96,4)	4	1488	1152	4.4	3.5	3.0	6.4	16.3	0.487	0.511	57.5
HB8-FN	HD-BS(11,4,96,8)	8	2976	2304	8.8	7.0	4.8	8.2	20.8	0.554	0.566	67.8
HB12-FN	HD-BS(11,4,96,12)	12	4464	3456	13.2	10.5	5.7	9.1	23.1	0.553	0.566	67.2
HB24-FN	HD-BS(11,4,96,24)	24	8928	6912	26.4	20.9	7.7	10.9	27.7	0.569	0.587	68.1
HB48-FN	HD-BS(11,4,96,48)	48	17856	13824	52.7	41.8	11.4	15.2	38.6	0.575	0.591	69.0
FloppyNet	HD-BS(11,4,96,N/A)	N/A	34848	0	105.4	0.0	15.1	18.2	46.2	0.554	0.568	67.3

256 × 256 pixel images with a cell size of 16 × 16 and a block size of 32 × 32, as suggested in [53].

Fig. 7 shows the EP score for all the considered methods. HB12-FN and FloppyNet performs equally well on the Combined dataset while on GardenPoints and Nordalnd the latter achieves slight higher EP. Our network outperforms by a substantial margin the other lightweight techniques: HOG, CALC, and CoHOG. VGG-16 captures the highest EP score in every environmental condition and on the Combined dataset. These results are not surprising considering the VGG-16’s large size and depth. However, VGG-16 requires 2.2s to compute an image descriptor, resulting in two orders of magnitude slower than any considered BNN. The complete set of T_i is reported in Table II while Fig. 8.A compares a selection of the most efficient techniques: the BNNs, CALC, and HOG. HB12-FN is the fastest one taking 9.1ms to process an image, 50% of FloppyNet’s inference time. Considering these two BNNs have similar VPR performance, our network represents a significant improvement over FloppyNet. The HOG implementation used for the experiments (OpenCV 4.5.0) can run only on a single thread. For a fair comparison, we reported the processing time of the proposed model for 1-thread (1T) execution using gray bars in Fig. 8.A. HOG takes about 7ms less than HB12-FN-1T to compute a descriptor. However, their VPR performance is very different. While HOG scores $EP = 0.318$, HB12-FN achieves 0.553. Such a performance gap corresponds to 28.6% less place correctly recognized in the Combined dataset (TP% column in Table II). We believe this gap is too wide to consider HOG as a good alternative to the proposed BNN.

B. Energy Usage

The energy usage, E_i , is reported in Table II and Fig. 8.B. E_i is determined using Eq. 12 from the average power usage measured directly from a RPI4 on 100 consecutive runs. RPI4 has an approximately continuous power usage during runtime. Thus, E_i is mainly influenced by the interference time and the number of active CPU cores. To this end, the processing time reduction due to HB-DS contributes to energy saving, which is essential for battery-supplied robotic platforms. The positive effect of HB-DS is well depicted by the energy difference between FloppyNet and HB12-FN as they differ only in the first stage. HOG is the most energy-

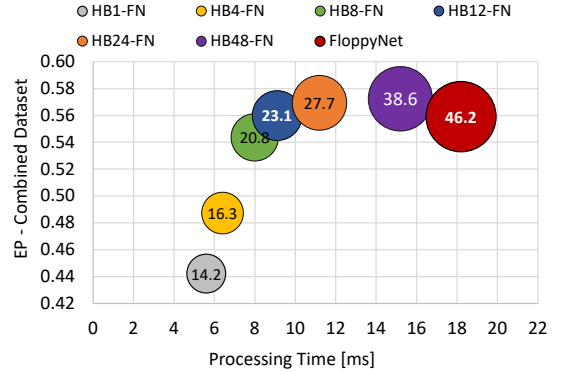


Fig. 9. EP score versus computational time for several depth multipliers. The circles’ area represents the energy usage in mJ per image processed.

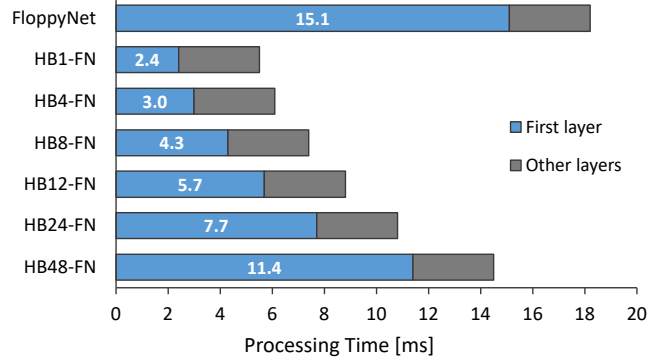


Fig. 10. Processing time for several depth multipliers. The blue bars represent the latency of the first layer while the gray bars indicate the rest of the network.

efficient technique. However, as motivated above, HOG has too low VPR performance to replace our best model.

C. Depth Multiplier as a Tuning Parameter

The HB-DS design enables the performance tuning of a BNN by acting only on the depth multiplier, d , without changing any other network parameter. Fig. 9 plots the EP score on the Combined dataset versus the processing time for several depth multipliers. The circles’ diameter represents the energy usage in mJ per processed image. HB12-FN, the model we selected for the comparison presented above,

reaches the same VPR performance as FloppyNet, spending one-half of the processing time and energy. Nevertheless, the VPR performance can be further improved by increasing d . For example, HB24-FN and HB48-FN outperform HB12-FN by a small margin at the cost of longer processing time and energy usage. If the target application has enough resources, HB24-FN and HB48-FN might be good options. On the opposite side, lower d values can find application in reducing a BNN's complexity to fit for extremely resource constraint hardware or saving energy to extend battery life. For example, the EP loss from HB12-FN to HB1-FN is 0.11, which corresponds to -14% correctly matched places in the Combined dataset (TP% in Table III). While HB12-FN is possibly the best option in many scenarios, HB1-FN might be preferred when energy saving is a strict requirement as it spends less energy than HB12-FN to process an image: 14.2 mJ against 23.1 mJ . It is worth mentioning that HB1-FN, which holds the worst VPR performance among our models, outperforms HOG, CALC and CoHOG while achieving higher computational efficiency (Tables II and III). Finally, Fig. 10 shows T_i for several depth multipliers. The blue bars represents the time spent on the first layer, which depends on d . The gray bars are for the rest of the layers. FloppyNet use a regular non-binary convolution as a first stage. The time spent on the first convolution is 84% of the entire processing time. The networks using HB-DS have a more fair distribution of the latency between the first and the other layers proving that our approach mitigates the bottleneck problem of BNNs.

VI. CONCLUSIONS

BNNs are an efficient class of deep neural networks using binary arithmetic to speed up convolutions. The slowest stage in a BNN is the first convolutional layer, non-binary for higher accuracy. This paper proposed a BNN achieving state-of-the-art VPR performance jointly with high computation and energy efficiency. Our network uses HB-DS, a module introduced in this paper, to address the latency bottleneck in the first stage of a BNN. HB-DS enables the performance tuning of a BNN by acting only on a single parameter to train models suitable for different deploy scenarios. An extension of this work is investigating HB-DS for different network architectures (e.g. ResNet) and different tasks than image matching, such as object detection and image segmentation.

REFERENCES

- [1] CoHOG source code. https://github.com/MubarizZaffar/VPR-Bench/tree/main/VPR_Techniques/CoHOG_Python. Accessed: 2021-11-06.
- [2] Raspberry Pi 4 Tech Specs. <https://www.raspberrypi.org/products/raspberry-pi-4-model-b/specifications/>. Accessed: 2021-03-06.
- [3] Tensorflow Lite. <https://www.tensorflow.org/lite>. Accessed: 2021-03-05.
- [4] M. Alizadeh, J. Fernández-Marqués, N. D. Lane, and Y. Gal. An empirical study of binary neural networks' optimisation. In *International Conference on Learning Representations*, 2019.
- [5] R. Arandjelovic, P. Gronat, A. Torii, T. Pajdla, and J. Sivic. Netvlad: CNN architecture for weakly supervised place recognition. In *Proceedings of the IEEE Conference on Computer Vision and Pattern Recognition*, pages 5297–5307, 2016.

- [6] B. Arcanjo, B. Ferrarini, M. Milford, K. D. McDonald-Maier, and S. Ehsan. An efficient and scalable collection of fly-inspired voting units for visual place recognition in changing environments. *IEEE Robotics and Automation Letters*, 7(2):2527–2534, 2022.
- [7] D. Bai, C. Wang, B. Zhang, X. Yi, and X. Yang. Sequence searching with cnn features for robust and fast visual place recognition. *Computers & Graphics*, 70:270–280, 2018.
- [8] T. Bannink, A. Hillier, L. Geiger, T. de Bruin, L. Overweel, J. Neeven, and K. Helwegen. Larq compute engine: Design, benchmark, and deploy state-of-the-art binarized neural networks, 2020.
- [9] Y. Bengio, N. Léonard, and A. C. Courville. Estimating or propagating gradients through stochastic neurons for conditional computation. *CoRR*, abs/1308.3432, 2013.
- [10] M. Chancán, L. Hernandez-Nunez, A. Narendra, A. B. Barron, and M. Milford. A hybrid compact neural architecture for visual place recognition. *IEEE Robotics and Automation Letters*, 5(2):993–1000, 2020.
- [11] Z. Chen, A. Jacobson, N. Sünderhauf, B. Upcroft, L. Liu, C. Shen, I. Reid, and M. Milford. Deep learning features at scale for visual place recognition. In *2017 IEEE International Conference on Robotics and Automation (ICRA)*, pages 3223–3230. IEEE, 2017.
- [12] Z. Chen, F. Maffra, I. Sa, and M. Chli. Only look once, mining distinctive landmarks from convnet for visual place recognition. In *2017 IEEE/RSJ International Conference on Intelligent Robots and Systems (IROS)*, pages 9–16. IEEE, 2017.
- [13] M. Courbariaux and Y. Bengio. Binarynet: Training deep neural networks with weights and activations constrained to +1 or -1. *CoRR*, abs/1602.02830, 2016.
- [14] M. Courbariaux, Y. Bengio, and J.-P. David. Training deep neural networks with low precision multiplications. *arXiv e-prints*, pages arXiv-1412, 2014.
- [15] N. Dalal and B. Triggs. Histograms of oriented gradients for human detection. In *2005 IEEE Computer Society Conference on Computer Vision and Pattern Recognition (CVPR'05)*, volume 1, pages 886–893 vol. 1, 2005.
- [16] B. Dongdong, W. Chaoqun, B. Zhang, Y. Xiaodong, Y. Xuejun, et al. CNN feature boosted seqslam for real-time loop closure detection. *Chinese Journal of Electronics*, 27(3):488–499, 2018.
- [17] S. K. Esser, J. L. McKinstry, D. Bablani, R. Appuswamy, and D. S. Modha. Learned step size quantization. *CoRR*, abs/1902.08153, 2019.
- [18] B. Ferrarini, M. Milford, K. D. McDonald-Maier, and S. Ehsan. Binary neural networks for memory-efficient and effective visual place recognition in changing environments. *IEEE Transactions on Robotics*, PREPRINT on ArXiv, Accepted Jan 2022.
- [19] B. Ferrarini, M. Waheed, S. Waheed, S. Ehsan, M. Milford, and K. D. McDonald-Maier. Visual place recognition for aerial robotics: Exploring accuracy-computation trade-off for local image descriptors. In *2019 NASA/ESA Conference on Adaptive Hardware and Systems (AHS)*, pages 103–108. IEEE, 2019.
- [20] B. Ferrarini, M. Waheed, S. Waheed, S. Ehsan, M. J. Milford, and K. D. McDonald-Maier. Exploring performance bounds of visual place recognition using extended precision. *IEEE Robotics and Automation Letters*, 5(2):1688–1695, April 2020.
- [21] L. Geiger and P. Team. Larq: An open-source library for training binarized neural networks. *Journal of Open Source Software*, 5(45):1746, 2020.
- [22] S. Han, J. Pool, J. Tran, and W. J. Dally. Learning both weights and connections for efficient neural networks. In *Proceedings of the 28th International Conference on Neural Information Processing Systems-Volume 1*, pages 1135–1143, 2015.
- [23] B. Hassibi and D. G. Stork. Second order derivatives for network pruning: optimal brain surgeon. In *Proceedings of the 5th International Conference on Neural Information Processing Systems*, pages 164–171, 1992.
- [24] Y. Hou, H. Zhang, and S. Zhou. Convolutional neural network-based image representation for visual loop closure detection. In *2015 IEEE International Conference on Information and Automation*, pages 2238–2245, 2015.
- [25] A. G. Howard, M. Zhu, B. Chen, D. Kalenichenko, W. Wang, T. Weyand, M. Andreetto, and H. Adam. Mobilenets: Efficient convolutional neural networks for mobile vision applications. *CoRR*, abs/1704.04861, 2017.
- [26] I. Hubara, M. Courbariaux, D. Soudry, R. El-Yaniv, and Y. Bengio. Quantized neural networks: Training neural networks with low pre-

- cision weights and activations. *The Journal of Machine Learning Research*, 18(1):6869–6898, 2017.
- [27] S. Ioffe and C. Szegedy. Batch normalization: Accelerating deep network training by reducing internal covariate shift. In *International Conference on Machine Learning*, pages 448–456, 2015.
- [28] H. Jégou, M. Douze, C. Schmid, and P. Pérez. Aggregating local descriptors into a compact image representation. In *CVPR 2010-23rd IEEE Conference on Computer Vision & Pattern Recognition*, pages 3304–3311. IEEE Computer Society, 2010.
- [29] A. Khaliq, S. Ehsan, Z. Chen, M. Milford, and K. McDonald-Maier. A holistic visual place recognition approach using lightweight cnns for significant viewpoint and appearance changes. *IEEE Transactions on Robotics*, pages 1–9, 2019.
- [30] A. Krizhevsky, I. Sutskever, and G. E. Hinton. Imagenet classification with deep Convolutional Neural Networks. In *Advances in neural information processing systems*, pages 1097–1105, 2012.
- [31] M. M. Larsson, E. Stenborg, L. Hammarstrand, M. Pollefeys, T. Sattler, and F. Kahl. A cross-season correspondence dataset for robust semantic segmentation. In *2019 IEEE/CVF Conference on Computer Vision and Pattern Recognition (CVPR)*, pages 9524–9534. IEEE, 2019.
- [32] Y. LeCun, J. S. Denker, and S. A. Solla. Optimal brain damage. In *Advances in neural information processing systems*, pages 598–605, 1990.
- [33] S. Lowry, N. Sünderhauf, P. Newman, J. J. Leonard, D. Cox, P. Corke, and M. J. Milford. Visual place recognition: A survey. *IEEE Transactions on Robotics*, 32(1):1–19, 2015.
- [34] F. Maffra, Z. Chen, and M. Chli. Viewpoint-tolerant place recognition combining 2d and 3d information for uav navigation. In *2018 IEEE International Conference on Robotics and Automation (ICRA)*, pages 2542–2549. IEEE, 2018.
- [35] F. Maffra, L. Teixeira, Z. Chen, and M. Chli. Real-time wide-baseline place recognition using depth completion. *IEEE Robotics and Automation Letters*, 2019.
- [36] N. Merrill and G. Huang. Lightweight unsupervised deep loop closure. In *Proceedings of Robotics: Science and Systems*, Pittsburgh, Pennsylvania, June 2018.
- [37] M. J. Milford and G. F. Wyeth. Seqslam: Visual route-based navigation for sunny summer days and stormy winter nights. In *2012 IEEE International Conference on Robotics and Automation*, pages 1643–1649. IEEE, 2012.
- [38] A. Pappalardo. Xilinx/brevitas. <https://doi.org/10.5281/zenodo.3333552>.
- [39] J. Philbin, O. Chum, M. Isard, J. Sivic, and A. Zisserman. Object retrieval with large vocabularies and fast spatial matching. In *2007 IEEE Conference on Computer Vision and Pattern Recognition*, pages 1–8. IEEE, 2007.
- [40] M. Rastegari, V. Ordonez, J. Redmon, and A. Farhadi. Xnor-net: Imagenet classification using binary convolutional neural networks. In *European conference on computer vision*, pages 525–542. Springer, 2016.
- [41] O. Russakovsky, J. Deng, H. Su, J. Krause, S. Satheesh, S. Ma, Z. Huang, A. Karpathy, A. Khosla, M. Bernstein, A. C. Berg, and L. Fei-Fei. ImageNet Large Scale Visual Recognition Challenge. *International Journal of Computer Vision (IJCV)*, 115(3):211–252, 2015.
- [42] D. Saad and E. Marom. Training feed forward nets with binary weights via a modified chir algorithm. *Complex Systems*, 4(5), 1990.
- [43] L. Sifre and P. S. Mallat. Rigid-motion scattering for image classification author. *English. Supervisor: Prof. Stéphane Mallat. Ph. D. Thesis. Ecole Polytechnique*, 2014.
- [44] T. Simons and D.-J. Lee. A review of binarized neural networks. *Electronics*, 8(6):661, 2019.
- [45] K. Simonyan and A. Zisserman. Very deep convolutional networks for large-scale image recognition. In *International Conference on Learning Representations*, 2015.
- [46] S. Skrede. Nordlandsbanen: minute by minute, season by season <https://nrkbeta.no/2013/01/15/nordlandsbanen-minute-by-minute-season-by-season/>. Accessed: 2021-11-06.
- [47] N. Sünderhauf, S. Shirazi, F. Dayoub, B. Upcroft, and M. Milford. On the performance of convnet features for place recognition. In *2015 IEEE/RSJ International Conference on Intelligent Robots and Systems (IROS)*, pages 4297–4304, 2015.
- [48] W. Tang, G. Hua, and L. Wang. How to train a compact binary neural network with high accuracy? In *Thirty-First AAAI conference on artificial intelligence*, 2017.
- [49] G. Toliás, R. Sicre, and H. Jégou. Particular Object Retrieval With Integral Max-Pooling of CNN Activations. In *ICLR 2016, International Conference on Learning Representations*, pages 1–12, San Juan, Puerto Rico, May 2016.
- [50] M. Waheed, M. Milford, K. McDonald-Maier, and S. Ehsan. Improving visual place recognition performance by maximising complementarity. *IEEE Robotics and Automation Letters*, 6(3):5976–5983, 2021.
- [51] M. Zaffar, S. Ehsan, M. Milford, and K. McDonald-Maier. Cohog: A light-weight, compute-efficient, and training-free visual place recognition technique for changing environments. *IEEE Robotics and Automation Letters*, 5(2):1835–1842, 2020.
- [52] M. Zaffar, S. Ehsan, M. Milford, and K. D. McDonald-Maier. Memorable maps: A framework for re-defining places in visual place recognition. *IEEE Transactions on Intelligent Transportation Systems*, pages 1–15, 2020.
- [53] M. Zaffar, S. Garg, M. Milford, J. Kooij, D. Flynn, K. McDonald-Maier, and S. Ehsan. Vpr-bench: An open-source visual place recognition evaluation framework with quantifiable viewpoint and appearance change. *International Journal of Computer Vision*, pages 1–39, 2021.
- [54] M. Zaffar, A. Khaliq, S. Ehsan, M. Milford, and K. McDonald-Maier. Levelling the playing field: A comprehensive comparison of visual place recognition approaches under changing conditions. In *IEEE ICRA Workshop on Dataset Generation and Benchmarking of SLAM Algorithms for Robotics and VR/AR*. IEEE, 2019.
- [55] B. Zhou, A. Lapedriza, A. Khosla, A. Oliva, and A. Torralba. Places: A 10 million image database for scene recognition. *IEEE transactions on pattern analysis and machine intelligence*, 40(6):1452–1464, 2017.